Fano resonance in transport through a mesoscopic two-lead ring

Khee-Kyun Voo and Chon Saar Chu
Department of Electrophysics, National Chiao Tung University, Hsinchu 300, Taiwan, Republic of China
(Received 15 March 2005; revised manuscript received 19 July 2005; published 4 October 2005)

The ballistic transport through a one-dimensional two-lead ring at zero magnetic field is studied. We have focused on the case in which the potential in the ring does not define closed cavities or dots. Even in the absence of well-defined quasibound states, we find Fano profiles in the transmission probability. Those Fano profiles appear at energies corresponding to the standing-wave states in the ring, but their occurrence depends sensitively on the commensurability of the system parameters. When the system parameters are commensurate, the widths of the profiles at some energies are infinitesimally small. These findings suggest that the conventional understanding of the Fano profiles as a result of the interference effect of the transition through resonant states and nonresonant continuum of states, might not account for all the Fano profiles seen in the transport measurements. Moreover, the sensitivity and tunability of the resonance with respect to the system parameters may be usable in the fabrication of electrical nanodevices.

DOI: 10.1103/PhysRevB.72.165307 PACS number(s): 73.23.Ad, 73.63.Kv

I. INTRODUCTION

The Fano resonance or profile is conventionally understood as a result of the interference between resonant and nonresonant processes. It was first observed and studied in nuclear physics[1] and atomic physics,[2] and later the effect was also observed in a wide variety of spectroscopy such as atomic photoionization,[3] optical absorption,[4] Raman scattering,[5] and also the scanning tunneling through a surface impurity atom.[6,7] As recent progress in the fabrication technology of electrical nanodevices has achieved devices of the size of the order of the various coherence lengths of the conduction electron, quantum mechanical effect and hence the Fano resonance has also been seen in mesoscopic systems. For instance, it is seen in the transport through systems which contain quantum dots[8–13] and carbon nanotubes.[14] Moreover, it is proposed that the resonance can be used in the probe of the phase coherency of the electrons in transport[15,16] and the design of mesoscopic spin filters.[17]

Most studies of the Fano resonance in the electronic transport have been along the conventional line, i.e., Fano profiles are attributed to well-defined quasibound states which are in degenerate and mixed with a continuum of states. For instance, an attractive impurity or a quantum dot (QD) is coupled to a quasi-one-dimensional (quasi-1D) transport channel,[18–20] a QD is placed on a one-dimensional (1D) or quasi-1D ring connected to two leads,[12,21–29] etc. In the case of a quasi-1D transport channel with an attractive impurity, some of the quasibound levels are degenerate, with the continuums of states due to the subbands below (e.g., see Ref. 18), and therefore an electron can either seep through the impurity level or bypass it via the band continuums. It is noted that no Fano resonance can be found in singly connected 1D systems,[18] since resonant and nonresonant processes can never coexist in transport due to the topology. In the above-mentioned cases, the problem is essentially the problem of a single impurity that is embedded into a continuum of states, which was well studied by Fano.[2] Nevertheless, similar asymmetric Fano profiles are also theoretically[30–32] and experimentally[8,9] seen in the transport in systems containing only open resonant cavities. Furthermore, in theoretical study, the width of the resonance can be sensitive to the potential in the resonant cavity and can even be tuned to approach *zero*. In those cases, the problem would not be readily understandable in the conventional scheme due to Fano.[2] By this, we mean a closed cavity or dot by a cell isolated by repulsive potential barriers or constrictions in the channels, else it is an open resonant cavity.

In order to gain understanding of the Fano profile in a transport that has unusual sharpness at no well-defined quasibound state, we explore the resonance in a 1D, but doubly connected system at zero magnetic field. The system has a topology the same as that of the frequently studied Aharonov-Bohm ring, with[12,21–28] and without[33] a QD on one of the arms, but we have focused on the case in which the potential defines only open resonant cavities in the ring. The choice of this system for our study is based on the fact that this is the simplest system that shows Fano resonance at no well-defined quasibound state, and the resonance width can also be sensitively tuned by the potential and can become infinitely sharp or collapse. It is hoped that due to the simplicity of this system more of the nature of the occurrence of the resonance beyond the conventional Fano's scheme[2] can be revealed. We have found that when the system parameters are *commensurate*, the Fano profiles at some energies can become infinitesimally sharp. We also have ventured to relate the commensurability to the constructive interference along the paths. The system parameters are, e.g., the location of the impurity potential and the arm lengths of the ring. There are also theoretical reports of the collapse of the Fano resonance[32,34,35] analogous to ours, but these reports are either on more complicated systems[32,35] or the collapsing behavior is not discussed.[34]

In Sec. II we present our formulation, and in Sec. III we present and discuss the results in several cases. We focus on systems with only repulsive and pointlike δ potentials. The idealized δ-potential model makes sense at the long-wavelength regime, and it also facilitates analytical analyses. Two aspects of the systems, open resonant cavity and commensurate system parameters, are highlighted, and the occur-

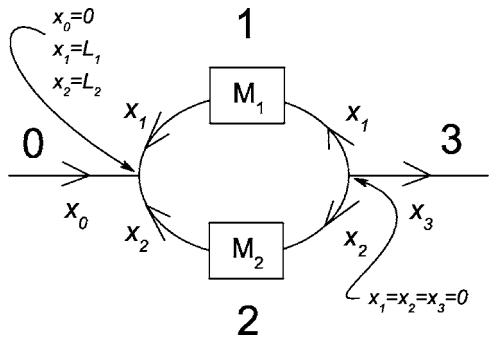

FIG. 1. The system we consider is a ring (with arms labeled by 1 and 2) connected to two leads (labeled by 0 and 3). The boxes on the ring labeled by $\mathbf{M}_{1,2}$ represent the scatterers on the arms. A coodinate system x_i is defined for the line segment labeled by i ($i=0$, 1, 2, and 3). While the arrows denote the positive direction of the coordinates, the right Y junction is defined at $x_1=x_2=x_3=0$, and the left Y junction is at $x_0=0$, $x_1=L_1$, and $x_2=L_2$.

rence and collapse of the Fano resonance are investigated. In the last section, Sec. IV, we give some remarks on our findings.

II. FORMULATION

We consider the ballistic transport through a two-lead ring as shown in Fig. 1. Both the ring and leads are considered as 1D, an approximation that is valid when the transverse dimension of the channel is narrow enough to allow only the lowest subband to be involved in the transport process. On each arm of the ring we include a scattering potential that is described by a transfer matrix $\mathbf{M}_i$, where $i=1,2$ labels the arm, and the wave functions on the opposite sides of a scatterer are connected by $\mathbf{M}_i$. At the three-leg junctions or Y junctions, the wave functions on the branches are connected via the Griffith's boundary condition[36] which we will describe shortly. The overall wave function can thus be found and the transmission probability be obtained.

At a given energy $E(>0)$, the wave function on each line segment in Fig. 1 can be expanded by the forward and backward traveling waves[34,37–43] as

$$\phi_i = A_i e^{ikx_i} + B_i e^{-ikx_i}, \quad i=0,1,2,\text{and } 3,$$

$$\phi_{i'} = A_i' e^{ikx_i} + B_i' e^{-ikx_i}, \quad i=1 \text{ and } 2, \tag{1}$$

where $\phi_{1',2'}$ are the wave functions before the scatterers and $\phi_{1,2}$ are after the scatterers, $k \equiv \sqrt{2mE}/\hbar$, and m is the effective mass of the traveling particle. The lengths of the arms of the ring are chosen as $L_{1,2}$ and the coordinate systems are as defined in Fig. 1. Across the scatterers, the continuity of the wave functions and their derivatives can be written as

$$\begin{bmatrix} A_1 \\ B_1 \end{bmatrix} = \mathbf{M}_1 \begin{bmatrix} A_1' \\ B_1' \end{bmatrix} \tag{2}$$

and

$$\begin{bmatrix} A_2 \\ B_2 \end{bmatrix} = \mathbf{M}_2 \begin{bmatrix} A_2' \\ B_2' \end{bmatrix}. \tag{3}$$

At the Y junctions the wave function continuity requirement[44] and Griffith's unitarity boundary condition[45] demand that the wave functions are jointed at the left Y junction by

$$A_0 + B_0 = A_1 e^{ikL_1} + B_1 e^{-ikL_1}, \tag{4}$$

$$A_0 + B_0 = A_2 e^{ikL_2} + B_2 e^{-ikL_2}, \tag{5}$$

$$(A_0 - B_0) + (A_1 e^{ikL_1} - B_1 e^{-ikL_1}) + (A_2 e^{ikL_2} - B_2 e^{-ikL_2}) = 0, \tag{6}$$

and at the right Y junction by

$$A_3 + B_3 = A_1' + B_1', \tag{7}$$

$$A_3 + B_3 = A_2' + B_2', \tag{8}$$

$$(A_3 - B_3) + (A_1' - B_1') + (A_2' - B_2') = 0. \tag{9}$$

The Griffith's boundary condition guarantees the net current flowing into a junction is zero. Since we consider particles incident from the left, we set $A_0=1$ and $B_3=0$. Equations (2)–(9) then constitute an equation set with ten linear equations and ten unknowns. It can then be solved, and the transmission probability $T=|A_3|^2$ be found. The transmission amplitude A_3 is found to be

$$A_3 = \frac{C}{D},$$

$$C \equiv e^{ikL_1}(\mathbf{M}_1^{11} - \mathbf{M}_1^{12}) + e^{-ikL_1}(\mathbf{M}_1^{21} - \mathbf{M}_1^{22}) + (L_1 \leftrightarrow L_2 \text{ and } \mathbf{M}_1 \leftrightarrow \mathbf{M}_2),$$

$$D \equiv 1 - \frac{1}{8}e^{ik(L_1+L_2)}(\mathbf{M}_1^{11}\mathbf{M}_2^{11} - 3\mathbf{M}_1^{12}\mathbf{M}_2^{12} + 2\mathbf{M}_1^{11}\mathbf{M}_2^{12}) + \frac{3}{8}e^{-ik(L_1+L_2)}(\mathbf{M}_1^{21}\mathbf{M}_2^{21} - 3\mathbf{M}_1^{22}\mathbf{M}_2^{22} + 2\mathbf{M}_1^{21}\mathbf{M}_2^{22}) + \frac{1}{4}e^{ik(L_1-L_2)}[(\mathbf{M}_1^{11} + \mathbf{M}_1^{12})(\mathbf{M}_2^{21} + \mathbf{M}_2^{22}) - 4\mathbf{M}_1^{12}\mathbf{M}_2^{22}] + (L_1 \leftrightarrow L_2 \text{ and } \mathbf{M}_1 \leftrightarrow \mathbf{M}_2), \tag{10}$$

where we have used the fact that $\det \mathbf{M}_i = 1$ (see, e.g., the discussion in Ref. 46). As the analytic expressions are cumbersome, most of the time we will proceed with our discussion by plotting out the numerical values only.

III. NUMERICAL RESULT

The behaviors of the transmission probability in some representative cases are studied in the following sections. We will focus on the dip and peak-dip profiles in the spectra, particularly, how they can occur or collapse when the system

parameters are tuned. Mathematically, we will see that the occurrence and collapse are related to the zeroes in the numerator C and denominator D in the transmission amplitude A_3 in Eq. (10). In turn, these zeroes are seen to be related to the standing-wave resonance (SWR) and two-path interference (2PI) in the arms of the ring.

A. Unequal arm lengths

In this section we investigate the case in which the arms and the leads are all at equipotential, but the arms have different lengths of L_1 and L_2. This setup is described by $\mathbf{M}_1=\mathbf{M}_2=1$ and the transmission amplitude A_3 in Eq. (10) becomes

$$A_3=\frac{i(\sin kL_1+\sin kL_2)}{1-\exp[-ik(L_1+L_2)]-\frac{1}{4}[\cos k(L_1+L_2)-\cos k(L_1-L_2)]}. \tag{11}$$

Total reflection may occur when the numerator in Eq. (11) vanishes. This requires $k(L_1-L_2)=(\text{odd integer})\times\pi$ or $k(L_1+L_2)=(\text{even integer})\times\pi$. The former equation is easily seen to correspond to a perfectly destructive 2PI between the arms. The latter equation is also easily seen to correspond to a standing wave on an isolated ring with circumference L_1+L_2. Thus it is seen that though the ring is coupled to the leads, the standing-wave states in the ring may still play a role in the transport through the ring. Note also that the SWR occurs without a red shift, in contrary to what one might expect in an open system. For a wave number k which corresponds to a perfectly destructive 2PI, the denominator in Eq. (11) is always found to be nonvanishing, and therefore there is always a total reflection under this condition. For a k in the SWR condition, the denominator in Eq. (11) vanishes if it happens that $k(L_1-L_2)=(\text{even integer})\times\pi$, which is the condition for a perfectly constructive 2PI between the two arms, and this can happen when L_2/L_1 is a rational number. When a k meets the perfectly constructive 2PI condition, the first order zeroes in the numerator and denominator in Eq. (11) cancel each other and give a nonvanishing transmission probability, which is unity. In short, when a k meets the SWR condition in the ring, a total reflection occurs when the k does not simultaneously meet a perfectly constructive 2PI condition. Otherwise, there is a perfect transmission. On the other hand, a total reflection always occurs at perfectly destructive 2PI. The above findings can be summarized into the following mathematical statements. Given a L_2/L_1, a total reflection must occur at $kL_1=(\text{odd integer})\times\pi(1-L_2/L_1)^{-1}$ (which corresponds to a perfectly destructive 2PI). A total reflection can also occur at $kL_1=2n\pi(1+L_2/L_1)^{-1}$, where n is an integer (which corresponds to a SWR in the ring), if $2n(1+L_2/L_1)^{-1}$ is not an integer. Otherwise, there is a perfect transmission. Note that $2n(1+L_2/L_1)^{-1}$ is always an integer when $L_1=L_2$ or $L_2=0$.

The above findings can be illustrated by concrete examples. Figure 2 shows the wave number dependence of the transmission probability for the case of almost equal arm lengths. It is seen that at equal arm lengths, though the transmission probability varies with the wave number, only total transmission is possible and there is no total reflection. This is because in any case there is no phase difference between the two paths and hence there is always a perfectly constructive 2PI. But at unequal arm lengths, total reflection is also seen to occur. The dips in the transmission probability[47] can be very sharp. At the limit $L_1=L_2$, the dips vanish by becoming infinitely sharp but not by recovering the transmission from zero. The spectrum does not progressively turn complicated when L_2/L_1 is detuned from 1. It becomes relatively neat when L_1 and L_2 are commensurate, i.e., when L_2/L_1 is a simple rational number and some of the resonance dips collapse. For instance, the case of $L_2/L_1\sim 2/3$ is depicted in Fig. 3. In Fig. 3 we see equally spaced sharper dips at $kL_1=2n\pi(1+L_2/L_1)^{-1}$ [provided that $2n(1+L_2/L_1)^{-1}$ is not an integer] due to the SWR in the ring. In addition, we also see equally spaced but smoother dips at $kL_1=(\text{odd integer})\times\pi(1-L_2/L_1)^{-1}$ due to the destructive 2PI. The 2PI effect has also resulted in a pronounced envelope in the transmission probability. The dips due to the SWR at $kL_1(2\pi)^{-1}\sim 3$ and 6 collapse when L_2/L_1 is exactly equal to $2/3$, i.e., when $kL_1/\pi=2n(1+L_2/L_1)^{-1}$ is exactly an integer. Interestingly, though the SWR results in transmission dips, around the dips the transmission is actually enhanced by the local minima of $|D|$ [see Fig. 2(d)]. The behaviors of the transmission probability is thus seen to be related to the interplay between the SWR and 2PI.

We have interpreted the behaviors of the numerator C and denominator D in Eq. (10) by the notions of SWR and 2PI. A closer look into the mathematical structures of them is also interesting. The very different natures of C and D can account for the abrupt occurrence and collapse of the transmission dips. Owing to the symmetry in the transfer matrices $\mathbf{M}_i^{11}=(\mathbf{M}_i^{22})^*$ and $\mathbf{M}_i^{12}=(\mathbf{M}_i^{21})^*$, $i=1,2$ (see, e.g., Ref. 46), C has always a constant phase regardless of the wave number and potential on the ring. Therefore, this phase can be peeled off and C will behave like a real-valued number; whereas D has a phase that depends on the wave number and potential, and it is genuinely a complex-valued number. Therefore, when a system parameter is slightly changed, the zeroes in C will only be slightly shifted and will remain, whereas zeroes in D can be abruptly lifted since they require both the real and imaginary parts to vanish simultaneously, which is a much more stringent condition. A nonzero transmission at delicately matched zeroes of C and D, e.g., the nonzero

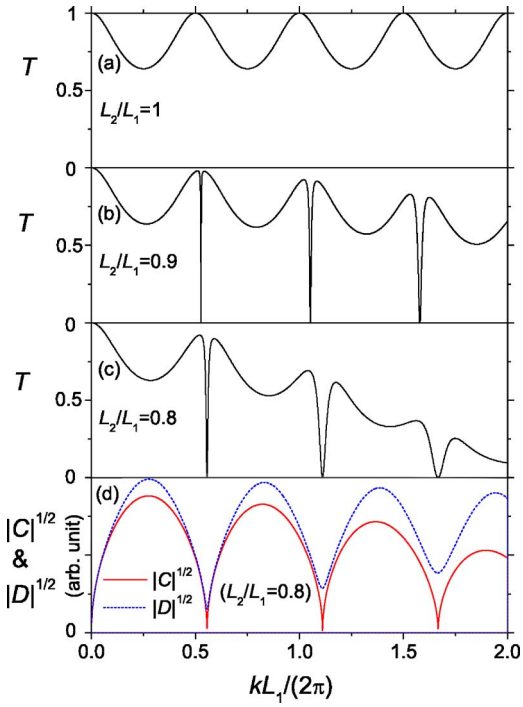

FIG. 2. (Color online) This figure shows that dips appear in the transmission probability T when L_1 and L_2 are slightly unequal. We have plotted T versus the dimensionless wave number $kL_1/(2\pi)$, for the case of no potential on the ring, and arm-length ratios L_2/L_1 =1, 0.9, and 0.8 [from (a) to (c)]. To illustrate the mathematical reason behind the formation of the transmission zeroes, the square roots of the magnitudes of the numerator C and denominator D [see Eq. (10)] of the transmission amplitude are plotted [in (d)] for the case of L_2/L_1=0.8. The zeroes in C are seen to remain but the zeroes in D (exist when $L_1=L_2$) are lifted, and hence give rise to T=0.

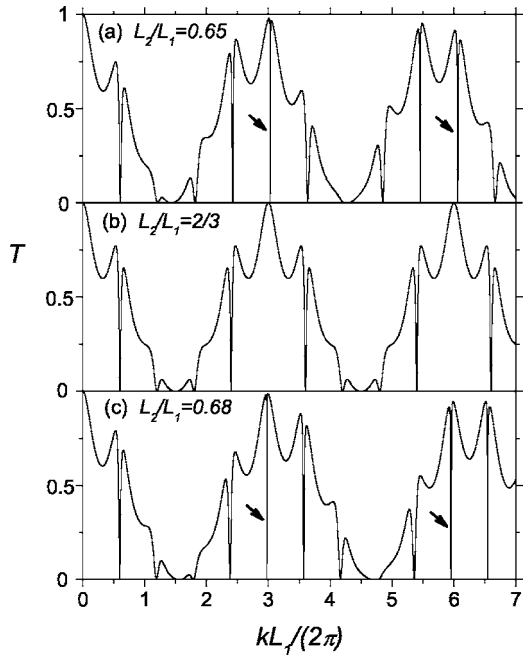

FIG. 3. For the case of no potential on the ring, the dips in the transmission probability T at some wave numbers are seen to become infinitely sharp or collapse when the arm lengths are commensurate. This figure shows T versus the dimensionless wave number $kL_1/(2\pi)$, for the case of no potential on the ring, and arm-length ratios L_2/L_1=0.65, 2/3, and 0.68 [from (a) to (c)]. The transmission dips at $kL_1/(2\pi)\sim$ 3 and 6 are seen to close at the limit L_2/L_1=2/3. Note also the transmission zeroes at $kL_1/(2\pi)$ $\sim$1.5 and 4.5, and the overall envelope due to the two-path interference.

transmission at $kL_1=n\pi$ in the case of $L_1=L_2$, is kind of "accidental." It is at a point of delicately matched SWR and perfectly constructive 2PI. It is very fragile and a slight detuning of an arm length can create a transmission zero (see Fig. 2). In later sections we will see that such behaviors of C and D are rather general and can abruptly create a Fano profile with a peak-dip pair when, e.g., the location of an impurity on the ring is shifted.

The above observation of the detuned zeroes in the numerator C and denominator D immediately implies that the numerical results can be casted into the Fano profile expression, and the dip's width can be explicitly related to the detuning from perfectly constructive 2PI. To be self-contained, we first give a very brief review of the Fano resonance. Consider a physical process which simultaneously involves a nonresonant part and a resonant part at energy ε =0. Let the nonresonant part be energy independent and described by a complex-valued amplitude t_0, and the resonant part be described by a complex-valued amplitude $t_r=za/(\varepsilon+ia)$, where z is a complex-valued number, and a is a real-valued number characterizing the width of the resonant process. The total transition amplitude $t_{tot}=t_0+t_r=t_0(\varepsilon+qa)/(\varepsilon+ia)$, where $q\equiv z/t_0+i$ is the Fano parameter, results in a total transition probability

$$T_{tot}=|t_0|^2\frac{|\varepsilon+qa|^2}{\varepsilon^2+a^2}. \tag{12}$$

Roughly speaking, in the case of $a\neq 0$ and $q\neq 0$, T_{tot} gives a dip (peak) when the numerator (denominator) in Eq. (12) is close to or equal to zero. When $a\neq 0$ and $q=0$, T_{tot} has only a dip at $\varepsilon=0$. The case of $a\neq 0$ and Im $q=0$ is discussed comprehensively in Fano's original paper.[2] In the case of $a\rightarrow 0$, the numerator and denominator in t_{tot} become exact zeroes at $\varepsilon=0$, but they are first order zeroes and cancel each other to give a finite transition probability. This is actually the case of commensurate arm lengths we have discussed. Since we know that a SWR dip can occur at $k=k_m$, where k_m is defined by $k_m(L_1+L_2)\equiv 2m\pi$, and m is an integer, we expand the transmission amplitude A_3 around a dip by letting $\delta\equiv(k-k_m)(L_1+L_2)$. Since we also know that a dip appears when $k_m(L_1-L_2)\neq 2n\pi$, where n is an integer, we define a detuning Δ from a perfectly constructive 2PI by $k_m(L_1-L_2)$ $\equiv 2n\pi+\Delta$, where Δ is within $[-\pi,+\pi]$ (note that given an m, n is determined). Then we expand A_3 at the vicinity of a dip when both the dimensionless parameters δ and Δ are small. We have expanded Eq. (11) for the case of max($|\delta|$) $\sim|\Delta|$ and $|\Delta|\ll\pi$. We expand the numerator to the third order and the denominator to the second order, and we obtain an approximate transmission amplitude

$$A_3 \simeq (-1)^{m+n}\left[1-\frac{1}{8}\Delta^2-\frac{1}{4}\frac{L_1-L_2}{L_1+L_2}\Delta\delta-\frac{1}{6}\frac{L_1^3+L_2^3}{(L_1+L_2)^3}\delta^2\right]\frac{\delta}{\delta+i\left\{\frac{1}{8}\Delta^2+\frac{1}{4}\frac{L_1-L_2}{L_1+L_2}\Delta\delta-\frac{1}{8}\left[5-\left(\frac{L_1-L_2}{L_1+L_2}\right)^2\right]\delta^2\right\}}. \quad (13)$$

The fraction part can be roughly viewed as a $q=0$ Fano profile with a δ-dependent width, and the other part can be viewed as a slow-varying envelope function. It is seen that within this range of δ the line shape is not in the usual Fano profile. But if we further restrict the range of δ to an order of magnitude smaller than Δ, i.e., $\max(|\delta|)\sim\Delta^2$, Eq. (13) can be simplified to

$$A_3 \simeq (-1)^{m+n}\left(1-\frac{\Delta^2}{8}\right)\frac{\delta}{\delta+i\frac{\Delta^2}{8}}, \quad (14)$$

i.e., near the minimum of a dip due to a SWR, the transmission probability profile is in the form of the $q=0$ Fano profile. Note that the parameter δ is a dimensionless wave number but not energy. When the SWR approaches a perfectly constructive 2PI (i.e., Δ approaches zero), the width of the dip ($\sim\Delta^2$) approaches zero and the dip vanishes. There are a few noteworthy points here. If one adopts the conventional understanding of the Fano profile with the notions of quasibound states and their lifetimes, the "lifetimes" of the "quasibound states" in our case might seem can be dramatically tuned by a slight tuning of an arm length. Moreover, the two arms of the ring are all the same except for their lengths, the SWR at $k(L_1+L_2)=2m\pi$ also occurs in the entire ring, and there is no obvious distinction between the "resonant" and "nonresonant" transition paths in our case.

On the other hand, we also have investigated the transmission amplitude A_3 for the case of $L_1=L_2=L$, in the complex wave number $\tilde{k}$ plane. This is a common way to investigate the nature of the quasibound states on the transition paths. In this special case of $L_1=L_2=L$, we can readily find poles at $\tilde{k}L=n\pi-i\ln 3$, where n is an integer. Though the $\mathrm{Re}\,\tilde{k}$ does correspond to a standing wave in an isolated ring with circumference $2L$, the $\mathrm{Im}\,\tilde{k}$ is large and comparable to the spacing in the $\mathrm{Re}\,\tilde{k}$. This indicates that these "quasibound" states are vaguely defined and this is in congruence with the fact that the ring is strongly coupled to the leads. It is therefore inappropriate to view these states as the quasibound states in Fano's original formulation.[2] But in contrary, transmission dips are seen and can be very sharp as soon as $L_1\neq L_2$. As we will see in the later sections, these standing-wave states are also related to the formation of the peak-dip pairs in the transmission probability when an impurity potential is added. It is thus seen that the conventional Fano resonance scheme with the notions of nonresonant and resonant transition paths, and lifetimes of the quasibound states, might be hard to provide a consistent understanding basis of the above results of equal arm lengths and slightly unequal arm lengths. This reveals the following logic. Though it is true that when there are resonant and nonresonant paths in a transition process there will be a Fano profile; the converse, when there is a Fano profile there are resonant and nonresonant transition paths in the transition process, may *not* be always true. In other words, though the mathematical form of the resulting transition probabilities can be unanimously in the Fano profile form as in Eq. (12), the underlying physical contents could be quite different.

B. With impurities

This section considers the case with a presence of point impurities on the ring. An impurity is described by a Dirac-δ function potential, and this model should apply to the case in which the extensions of the potentials are small compared with the wavelengths of the incident particles and the arm lengths of the ring. We first consider the case in which an impurity is embedded into arm 1, by adding the potential $V_1\delta(x_1-X_1)$, where V_1 is the strength of the impurity potential and X_1 is the location of the impurity in coordinate x_1 on arm 1. The corresponding transfer matrix is

$$\mathbf{M}_1=\begin{bmatrix}1-\frac{imV_1}{\hbar^2k} & -e^{-i2kX_1}\frac{imV_1}{\hbar^2k}\\ e^{i2kX_1}\frac{imV_1}{\hbar^2k} & 1+\frac{imV_1}{\hbar^2k}\end{bmatrix}. \quad (15)$$

Henceforth we will use the dimensionless parameter $v_1\equiv mL_1V_1/(2\pi\hbar^2)$ to characterize the impurity strength. It is noted that the transfer matrix has the symmetry $\mathbf{M}_1^{11}=(\mathbf{M}_1^{22})^*$ and $\mathbf{M}_1^{12}=(\mathbf{M}_1^{21})^*$. Arm 2 has no potential added and hence $\mathbf{M}_2=1$. A few more words on how to relate the dimensionless impurity strength v_1 to the experiments are worthwhile. A potential with a small spatial extension a and a magnitude of $\bar{V}_1$ can be approximated by a δ potential with $V_1=a\bar{V}_1$, and hence $v_1=mL_1\bar{V}_1a/(2\pi\hbar^2)$. For instance, if we have $m=m_{\mathrm{GaAs}}\simeq 0.067\,m_{\mathrm{bare}}$, $L_1=3\ \mu$m, and $a=0.03\ \mu$m, $v_1=1$ corresponds to $\bar{V}_1\simeq 0.08$ meV.

Figure 4 shows how the asymmetric Fano profile arises when the strength of a repulsive impurity on arm 1 grows. In Fig. 4 we have chosen $L_1=L_2$ and $X_1/L_1=0.3$. The peak-dip profile is in contrast with the mere dip profile in the no-impurity case in Sec. III A, but both of them are seen to develop from zero widths. Mathematically the dips are also due to the lift of zeroes in the denominator D [see Fig. 4(d)].

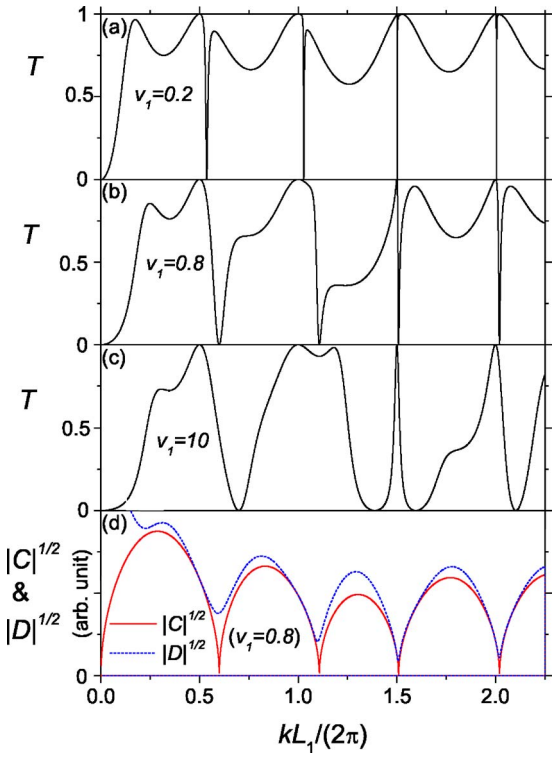

FIG. 4. (Color online) Asymmetric Fano profiles are seen in the transmission probability T when there is an impurity potential on the ring. We have plotted T versus the dimensionless wave number $kL_1/(2\pi)$ for the cases of $L_1=L_2$, an arbitrarily chosen impurity location $X_1/L_1=0.3$, and increasing potential strengths $v_1=0.2$, 0.8, and 10 (cutoff limit) [from (a) to (c)]. The Fano profiles are seen to evolve from the $v_1=0$ limit by increasing width. The square roots of the magnitudes of the numerator C and denominator D [see Eq. (10)] of the transmission amplitude are also plotted [in (d)] for the case of $v_1=0.8$ to illustrate how the Fano profiles are formed.

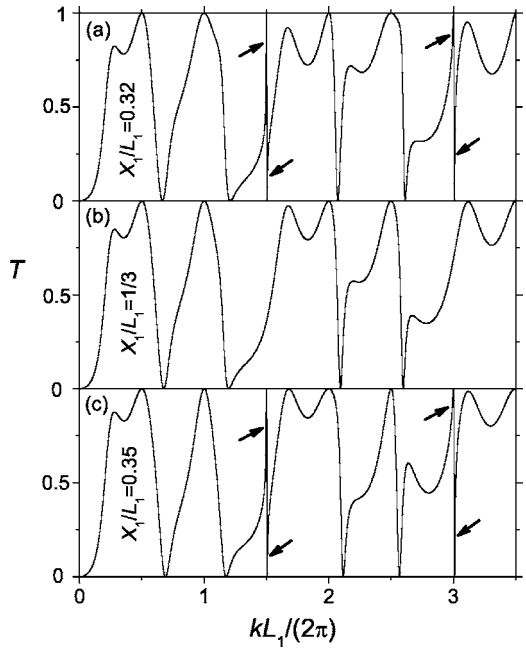

FIG. 5. Even at appreciable impurity strength, the Fano profiles in the transmission probability T at some wave numbers can collapse when the impurity is located commensurately. To illustrate this, we have plotted T versus the dimensionless wave number $kL_1/(2\pi)$ for the case of $L_1=L_2$, impurity strength $v_1=2$, and impurity locations $X_1/L_1=0.32$, $1/3$, and 0.35 [from (a) to (c)]. The Fano profiles at $kL_1/(2\pi)\sim 1.5$ and 3 are seen to collapse when the impurity is located at $X_1/L_1=1/3$.

It is noted that the dips are not necessarily at the eigenenergies of an isolated ring with a point impurity, since all the locations of the impurity and Y junctions have substantial effects on the standing waves in the ring. At the strong impurity limit [Fig. 4(c)], the zero transmission dips are wide and can also be analytically found to locate at $kX_1=\text{integer}\times\pi$ or $k(L_1-X_1)=\text{integer}\times\pi$. This agrees with the result of the transport through a 1D wire with a stub.[34] An arm is essentially cut off when the impurity on it is very strong, and the arrangement of our system for Fig. 4(c) is equivalent to a 1D wire with two stubs of lengths X_1 and L_1-X_1. There will be zero transmission when the length of any one of the stubs just matches an integral number of half-wavelengths.

Similar to the collapse of the dip profile in Sec. III A, the peak-dip profile here can also collapse. In Fig. 5 we have illustrated the phenomenon by showing the transmission probability for the case in which the impurity is on a special location on an arm. We have chosen $L_1=L_2$ and $X_1/L_1\sim 1/3$, and the resonant profiles at $kL_1/(2\pi)=1.5$ and 3 are seen to collapse when $X_1/L_1=1/3$. Though the formidable expressions of C and D forbid a detailed analytical analysis, it can be readily verified that at a k that simultaneously satisfies $kL_1=n_1\pi$, $kL_2=n_2\pi$, $kX_1=n_1'\pi$, where n_1, n_2, and n_1' are integers, and n_1+n_2 is even [i.e., $k(L_1+L_2)=\text{integer}\times 2\pi$], both C and D vanish but they give a nonzero transmission amplitude $A_3=C/D=(-1)^{n_1}[1+imV_1/(\hbar^2k)]^{-1}$. The above situation can arise when X_1/L_1 and L_2/L_1 are simple rational numbers. At such a mathematically "accidental" nonzero transmission, it is expected that a slight detuning of X_1 can generate a transmission zero such as in those cases discussed in Sec. III A. Note that the above-mentioned conditions for k imply that $k(L_1-L_2)=\text{integer}\times 2\pi$. Thus these conditions are seen to be similar to those in Sec. III A, and as we will see, the conditions for the collapse of the profiles in the two impurity case is also similar.

We can also obtain an approximate analytical expression for the transmission amplitude at the vicinity of a peak-dip profile when the impurity is at a location such that the profile is very sharp and about to collapse. The relationship between the resonance width and the detuning of the impurity location will then be more explicit. In our previous discussion, we have seen that if the ratios L_2/L_1 and X_1/L_1 are rational, the peak-dip profile at the wave number k_0 has a zero width, where k_0 is defined by $k_0L_1=n_1\pi$, $k_0L_2=n_2\pi$, n_1+n_2 is even, and $k_0X_1=n_1'\pi$. We therefore can make an expansion around k_0 for the case of a small detuning of the impurity location and the resonance has a very small width. As before, we let $k_0L_1=n_1\pi$, $k_0L_2=n_2\pi$, and n_1+n_2 is even, but now we let $k_0X_1=n_1'\pi+\Delta$. Defining a dimensionless wave number $\delta\equiv(k-k_0)(L_1+L_2)$, considering the regime of $\max(|\delta|)\sim\Delta^2$

and $|\Delta| \ll \pi$, and also assumming that $\tilde{v}_1 \equiv v_1/[(n_1+n_2)\pi]$ is at most of the order of 1, we can expand the numerator C and denominator D to obtain an approximate transmission amplitude A_3. To the lowest nonvanishing order,

$$A_3 \simeq \frac{(-1)^{n_1}}{1+i\tilde{v}_1} \frac{\delta - 2\tilde{v}_1\Delta^2}{\left[\delta - \dfrac{2\tilde{v}_1\Delta^2}{1+\tilde{v}_1^2}\right] + i\dfrac{2\tilde{v}_1^2\Delta^2}{1+\tilde{v}_1^2}}. \tag{16}$$

The zero of the numerator is seen to occur at $\delta = 2\tilde{v}_1\Delta^2$, while the zero of the real part of the denominator is seen to occur at $\delta = 2\tilde{v}_1\Delta^2/(1+\tilde{v}_1^2)$. The locations of the two zeroes do not coincide as long as $\tilde{v}_1$ and Δ are nonzero, and such situation of detuned zero locations corresponds to the case of a nonzero Fano parameter q. Since $(1+\tilde{v}_1^2) > 1$, when $\tilde{v}_1 > 0$ (the impurity is repulsive), the peak appears to precede the dip; if $\tilde{v}_1 < 0$ (the impurity is attractive), the order of appearance of the peak and dip is swapped. This property is probably usable in the design of mesoscopic spin filters. For instance, if the impurity potential is spin dependent, e.g., it is provided by a magnetic impurity or magnetic scanning tunneling microscopic tip, the transmission dip of the spin up (down) electrons may coincide with the transmission peak of the spin down (up) electrons. Therefore, at this incident energy, the device is a spin filter. The overall width of the resonance depends neither on the sign of the impurity potential ($\tilde{v}_1$) nor the detuning (Δ).

What we have learnt up to now is that the existence of SWR in the ring provides only the possibility of dip or peak-dip resonance in the transmission. Eventually, whether the resonance will occur or not is contingent on the commensurability of the system parameters. In the case of commensurate system parameters, some would-be dips which meet the condition of perfectly constructive 2PI will have infinitely small widths, and the resonances are removed. In contrast, the conventional Fano resonance[2] and Breit-Wigner (BW)[48] resonance are robust against slight tuning of the system parameters.

The case of two impurities on the ring resembles very much the cases of no impurity and one impurity. The Fano profile also collapses when it meets the perfectly constructive 2PI condition. We will consider the case of each arm with one impurity embedded. The impurity scatterings are described by $\mathbf{M}_1$ and $\mathbf{M}_2$, where $\mathbf{M}_1$ is the same as that in Eq. (15), and $\mathbf{M}_2$ is obtained from $\mathbf{M}_1$ by the substitution $X_1 \to X_2$ and $V_1 \to V_2$. $V_i (i=1,2)$ is the strength of an impurity, and X_i is the location of an impurity in the coordinate x_i on arm i. In such an arrangement, the two leads are always separated by the impurities. When both impurities are away from the Y junctions, the potential defines an open resonant cavity in the ring but not a closed dot. We will use the dimensionless parameter $v_i \equiv mL_1V_i(2\pi\hbar^2)^{-1}$ to characterize the strengths of the impurity potentials (note that we have used L_1 in the definitions of both v_1 and v_2).

Figure 6 shows the transmission probability for the cases of symmetric and asymmetric potentials on the arms. For a symmetric arrangement of the arms, i.e., $v_1 = v_2$, $X_1 = X_2$, and $L_1 = L_2$, only broad structures are seen. But when the potentials on the arms are asymmetric, e.g., either $X_1 \neq X_2$ or $v_1 \neq v_2$, Fano profiles are seen. The almost-perfect transmission peaks in the Fano profiles at low energies are rather surprising since the two leads are separated by the δ potentials on both arms. In a 1D system, there is no perfect transmission through a single δ-potential barrier at finite energy, whereas perfect transmission through a double δ-potential barrier at finite energy is possible, since the barriers create quasibound states in between them and BW resonant tunneling can take place. In our cases for Fig. 6, no region between the leads is enclosed by the repulsive potentials and therefore one usually does not expect any perfect transmission at finite energy. It is thus seen that the doubly connected 1D system behaves differently from the singly connected 1D system. The fact that the Fano profile appears only at asymmetric potentials on the arms indicates that the profiles are intimately related to the constructive 2PI between the arms. This is similar to the case in which $L_1 \simeq L_2$ but no potential is added onto the arms studied in Fig. 2.

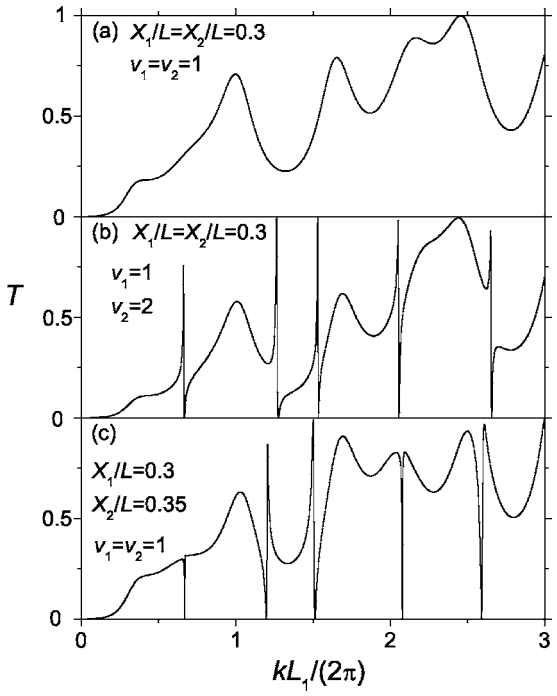

FIG. 6. Fano profiles are seen in the transmission probability T when the symmetricity of the two arms are disturbed. To illustrate this, we have plotted T versus the dimensionless wave number $kL_1/(2\pi)$ for the case of $L_1 = L_2 \equiv L$, and two impurities with strengths $v_{1,2}$ at $X_{1,2}$. The case of symmetric arms are illustrated by (a) $X_1/L = X_2/L = 0.3$ and $v_1 = v_2 = 1$; whereas the case of asymmetric impurity strengths are illustrated by (b) $X_1/L = X_2/L = 0.3$, $v_1 = 1$, and $v_2 = 2$; and the case of asymmetric impurity locations are illustrated by (c) $v_1 = v_2 = 1$, $X_1/L = 0.3$, and $X_2/L = 0.35$.

The collapse of the Fano profile also occurs in other cases, particularly in cases where the system parameters are commensurate. Figure 7 illustrates the collapse at a particular wave number using a system with $L_2/L_1 = 2/3$, $X_1/L_1 = 1/3$, and $X_2/L_2 \sim 1/2$. To work out rigorously all the wave numbers at which the collapse can occur would be difficult due to the complexity of C and D [see Eq. (10)], but an ansatz

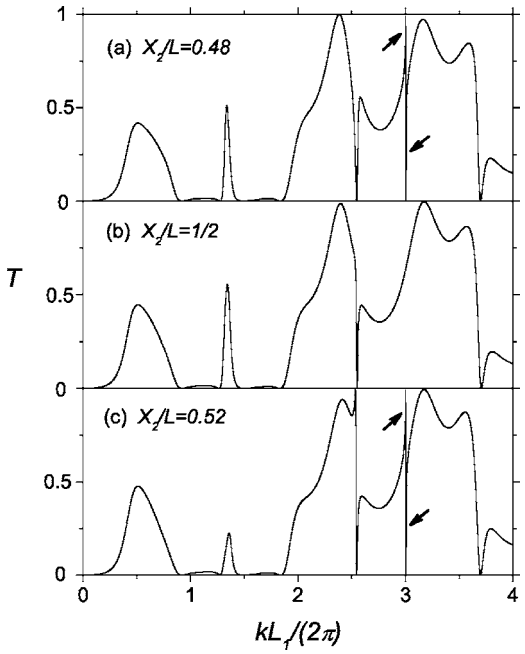

FIG. 7. Collapse of the Fano profile can also occur at more complicated system arrangements, as long as the system parameters are commensurate. For instance, we have plotted the transmission probability T versus the dimensionless wave number $kL_1/(2\pi)$ for the case in which $L_2/L_1=2/3$ and an impurity is placed on each arm. The strengths of the impurities on arms 1 and 2 are arbitrarily chosen as $v_1=1$ and $v_2=1.3$ respectively. The location of the impurity on arm 1 is chosen as $X_1/L_1=1/3$, while the location of the impurity on arm 2 is chosen as $X_2/L_2=0.48$, 1/2, and 0.52 [from (a) to (c)]. We note that the Fano profile at $kL_1/(2\pi)\sim 3$ collapses at approaching the commensurate location $X_2/L_2=1/2$.

similar to that in Sec. III B is seen to work well. It can be verified by direct substitution that at a k which simultaneously meets the conditions $kL_i=n_i\pi$, $kX_i=n_i'\pi$, where n_i and n_i' are integers $(i=1,2)$, and n_1+n_2 is even [i.e., $k(L_1+L_2)=(\text{even integer})\times\pi$], both C and D vanish, but the transmission amplitude $A_3=C/D=(-1)^{n_1}[1+im(V_1+V_2)/(\hbar^2k)]^{-1}$ is nonzero. Due to this mathematical structure, a zero transmission is anticipated at this k when any one of the system parameters, the impurity locations or arm lengths, is detuned. An illustration of the above mathematics is given in Fig. 7, and the resonance is seen to be a peak-dip pair. Since the above conditions for k also imply $k(L_1-L_2)=\text{integer}\times 2\pi$, which is a perfectly constructive 2PI, this again suggests that the phenomenon is related to the SWR and 2PI on the arms.

IV. CONCLUDING REMARKS

We have studied in this paper the ballistic transport through a 1D ring in the regime of a comparable particle's wavelength and a ring's dimension. In all cases, repulsive δ potentials are used, and no two δ potentials are placed on the same arm so that they do not create quasibound states. Nevertheless, a Fano profile can still be found and is shown to be related to the standing-wave states in the ring. The Fano profiles encountered in this paper grow or collapse by changing their widths, but not by changing their dips' depths or peaks' heights. We also have checked the case of attractive impurity potentials, and we have found that the results are qualitatively the same.[49]

In our study, several aspects of the Fano resonance are examined. Firstly, well-defined quasibound states which are weakly coupled to a continuum of states may not be necessary for the observation of the resonance. In other words, though the simultaneous presence of resonant and nonresonant processes in a physical process results in a Fano profile,[2] it might not be true to say that the observation of a Fano profile always implies the simultaneous presence of resonant and nonresonant processes in the underlying mechanism. Moreover, in our study the resonances are identified as the standing waves on the entire ring but not on only one of the arms (paths). Hence there is no clear distinction between the "resonant" and "nonresonant" paths. Secondly, commensurability is an important factor in the occurrence of the Fano profile. When the system parameters are commensurate, the Fano profiles at some energies can disappear by collapsing their widths to zero. Hence the presence of standing-wave resonance in the ring does not guarantee the occurrence of the Fano profile. Since the commensurability is found to be related to the constructive 2PI between the two arms, the width of the profile is seen to be controlled by the 2PI. While collapse of the Fano profile is also seen in the theoretical investigations of more complicated systems,[32,35] in the study of our exceedingly simple system, the collapse can be further seen as a result of the constructive 2PI. The abrupt occurence or collapse of the profile also indicates that the problem might not be equivalent to the conventional one discussed by Fano,[2] since a slight change in the system should not create or remove any quasibound states, or change their lifetimes dramatically. In our case, the prominent behaviors of the transmission probability are seen to be related to the SWR and 2PI. How the understanding of this simple system can be related or extended to the case of more complicated systems will be an interesting subject.

The sensitivity of the Fano profile to the device geometry and spatial details of the potential may imply that a naive tight-binding formulation of the quantum coherent device is not always viable. For instance, if a potential barrier is simply modeled by a hopping integral, or a resonance state is simply modeled by a zero-dimensional state, the spatial information of the device will be lost, and the consequences of the commensurability of the system parameters will be gone. We point out that such sensitivity of the resonance might be useful in the design of mesoscopic electrical switches, with the impurity potential provided by, e.g., a movable scanning tunneling microscopic tip.

We have left out some issues. For instance, the finite width of the transport channel has not been considered. We believe the Fano profile will be still present (e.g., see a related study in Ref. 50), and the question is just how it will be reshaped. Another issue is how the Fano profile will be affected by the inelastic dephasing process along the transport channel. These issues will be deferred to a later project.

ACKNOWLEDGMENTS

This work is supported by the NSC of Taiwan under Grant No. 93-2811-M-009-029. We thank C.-S. Tang and L.-Y. Wang for useful discussions, and the National Center for Theoretical Sciences (Physics Division) of Taiwan for letting us to use their facilities.

[1] R. K. Adair, C. K. Bockelman, and R. E. Peterson, Phys. Rev. **76**, 308 (1949).
[2] U. Fano, Phys. Rev. **124**, 1866 (1961).
[3] U. Fano and A. R. P. Rau, *Atomic Collision and Spectra* (Academic Press, Orlando, 1986).
[4] J. Faist, F. Capasso, C. Sirtori, K. W. West, and L. N. Pfeiffer, Nature (London) **390**, 589 (1997).
[5] F. Cerdeira, T. A. Fjeldly, and M. Cardona, Phys. Rev. B **8**, 4734 (1973).
[6] V. Madhavan, W. Chen, T. Jamneala, M. F. Crommie, and N. S. Wingreen, Science **280**, 567 (1998).
[7] J. Li, W.-D. Schneider, R. Berndt, and B. Delley, Phys. Rev. Lett. **80**, 2893 (1998).
[8] J. Gores, D. Goldhaber-Gordon, S. Heemeyer, M. A. Kastner, H. Shtrikman, D. Mahalu, and Y. Meirav, Phys. Rev. B **62**, 2188 (2000).
[9] I. G. Zacharia, D. Goldhaber-Gordon, G. Granger, M. A. Kastner, Y. B. Khavin, H. Shtrikman, D. Mahalu, and U. Meirav, Phys. Rev. B **64**, 155311 (2001).
[10] K. Kobayashi, H. Aikawa, S. Katsumoto, and Y. Iye, Phys. Rev. Lett. **88**, 256806 (2002).
[11] C. Fuhner, U. F. Keyser, R. J. Haug, D. Reuter, and A. D. Wieck, cond-mat/0307590 (unpublished).
[12] K. Kobayashi, H. Aikawa, A. Sano, S. Katsumoto, and Y. Iye, Phys. Rev. B **70**, 035319 (2004).
[13] M. Sato, H. Aikawa, K. Kobayashi, S. Katsumoto, and Y. Iye, cond-mat/0410062 (unpublished).
[14] J. Kim, J.-R. Kim, Jeong-O. Lee, J. W. Park, H. M. So, N. Kim, K. Kang, K.-H. Yoo, and J.-J. Kim, Phys. Rev. Lett. **90**, 166403 (2003).
[15] A. A. Clerk, X. Waintal, and P. W. Brouwer, Phys. Rev. Lett. **86**, 4636 (2001).
[16] Y.-J. Xiong and S.-J. Xiong, Int. J. Mod. Phys. B **16**, 1479 (2002).
[17] J. F. Song, Y. Ochiai, and J. P. Bird, Appl. Phys. Lett. **82**, 4561 (2003).
[18] E. Tekman and P. F. Bagwell, Phys. Rev. B **48**, 2553 (1993).
[19] J. U. Nockel and A. D. Stone, Phys. Rev. B **50**, 17415 (1994).
[20] A. C. Johnson, C. M. Marcus, M. P. Hanson, and A. C. Gossard, Phys. Rev. Lett. **93**, 106803 (2004).
[21] A. Yacoby, M. Heiblum, D. Mahalu, and H. Shtrikman, Phys. Rev. Lett. **74**, 4047 (1995).
[22] A. L. Yeyati and M. Buttiker, Phys. Rev. B **52**, R14360 (1995).
[23] G. Hackenbroich and H. A. Weidenmuller, Phys. Rev. Lett. **76**, 110 (1996).
[24] J. Wu, B.-L. Gu, H. Chen, W. Duan, and Y. Kawazoe, Phys. Rev. Lett. **80**, 1952 (1998).
[25] O. Entin-Wohlman, A. Aharony, Y. Imry, and Y. Levinson, cond-mat/0109328 (unpublished).
[26] K. Kobayashi, H. Aikawa, S. Katsumoto, and Y. Iye, Phys. Rev. B **68**, 235304 (2003).
[27] C. Benjamin and A. M. Jayannavar, Phys. Rev. B **68**, 085325 (2003).
[28] H. Aikawa, K. Kobayashi, A. Sano, S. Katsumoto, and Y. Iye, Phys. Rev. Lett. **92**, 176802 (2004).
[29] P. Singha Deo, Solid State Commun. **107**, 69 (1998).
[30] M. Mendoza and P. A. Schulz, Phys. Rev. B **68**, 205302 (2003).
[31] Y. Takagaki and K. H. Ploog, Phys. Rev. B **70**, 073304 (2004).
[32] V. A. Margulis and M. A. Pyataev, J. Phys.: Condens. Matter **16**, 4315 (2004).
[33] Y. Gefen, Y. Imry, and M. Ya. Azbel, Phys. Rev. Lett. **52**, 129 (1984).
[34] J.-B. Xia, Phys. Rev. B **45**, 3593 (1992).
[35] C. S. Kim, A. M. Satanin, Y. S. Joe, and R. M. Cosby, Phys. Rev. B **60**, 10962 (1999).
[36] J. Stanley Griffith, Trans. Faraday Soc. **49**, 345 (1953); **49**, 650 (1953).
[37] M. Buttiker, Y. Imry, and M. Ya. Azbel, Phys. Rev. A **30**, 1982 (1984).
[38] J. M. Mao, Y. Huang, and J. M. Zhou, J. Appl. Phys. **73**, 1853 (1993).
[39] M. V. Moskalets, Low Temp. Phys. **23**, 824 (1997).
[40] C.-M. Ryu and S. Y. Cho, Phys. Rev. B **58**, 3572 (1998).
[41] B. Molnar, F. M. Peeters, and P. Vasilopoulos, Phys. Rev. B **69**, 155335 (2004).
[42] B. Molnar, P. Vasilopoulos, and F. M. Peeters, cond-mat/0407536 (unpublished).
[43] D. Frustaglia and K. Richter, Phys. Rev. B **69**, 235310 (2004).
[44] The wave function continuity requirement demands $\phi_0=\phi_1=\phi_2$ at the left Y junction and $\phi_{1'}=\phi_{2'}=\phi_3$ at the right Y junction in Fig. 1.
[45] The Griffith's boundary condition states that at an n-leg junction, the sum of the spatial derivatives of the wave functions on the legs is zero, i.e., $\Sigma_i(\partial\phi_i/\partial x_i)=0$, where the directions of the coordinates are defined either simultaneously toward the junction or outward.
[46] G. Grosso and G. P. Parravicini, *Solid State Physics* (Academic Press, New York, 2000), p. 8.
[47] Such dips at unequal arm lengths were reported in Ref. 34, but no further discussion was made.
[48] G. Breit and E. Wigner, Phys. Rev. **49**, 519 (1936).
[49] K.-K. Voo and C. S. Chu (unpublished).
[50] A. A. Kiselev and K. W. Kim, J. Appl. Phys. **94**, 4001 (2003).